HHS Public Access

Author manuscript

Mol Psychiatry. Author manuscript; available in PMC 2016 August 23.

Published in final edited form as:

Mol Psychiatry. 2016 September ; 21(9): 1194–1201. doi:10.1038/mp.2016.5.

Predicting clinical outcome from reward circuitry function and white matter structure in behaviorally and emotionally dysregulated youth

Michele A. Bertocci, Ph.D.[1,*], **Genna Bebko, Ph.D.**[1,*], **Amelia Versace, M.D.**[1], **Jay C. Fournier, Ph.D.**[1], **Satish Iyengar, PhD**[2], **Thomas Olino**[3], **Lisa Bonar, B.S.**[1], **Jorge R. C. Almeida, M.D., Ph.D.**[4], **Susan B. Perlman, Ph.D.**[1], **Claudiu Schirda, Ph.D.**[1], **Michael J. Travis, M.D.**[1], **Mary Kay Gill, R.N., M.S.N.**[1], **Vaibhav A. Diwadkar, Ph.D.**[5], **Erika E. Forbes, Ph.D**[1], **Jeffrey L. Sunshine, M.D., Ph.D.**[6], **Scott K Holland, Ph.D.**[7], **Robert A. Kowatch, M.D., Ph.D.**[8], **Boris Birmaher, M.D.**[1], **David Axelson, M.D.**[1,8], **Sarah M. Horwitz, Ph.D.**[9], **Thomas W. Frazier, Ph.D.**[10], **L. Eugene Arnold, M. D., M.Ed.**[11], **Mary. A Fristad, Ph.D, ABPP**[11], **Eric A. Youngstrom, Ph.D.**[12], **Robert L. Findling, M.D, M.B.A.**[6,13], and **Mary L. Phillips, M.D., M.D. (Cantab)**[1]

[1]University of Pittsburgh Medical Center, University of Pittsburgh

[2]Department of Statistics, University of Pittsburgh

[3]Department of Psychology, Temple University

[4]Alpert Medical School, Brown University

[5]Department of Psychiatry and Behavioral Neuroscience, Wayne State University

[6]University Hospitals Case Medical Center/Case Western Reserve University

[7]Cincinnati Children's Hospital Medical Center, University of Cincinnati

[8]The Research Institute at Nationwide Children's Hospital

[9]Department of Child Psychiatry, New York University School of Medicine

[10]Pediatric Institute, Cleveland Clinic

[11]Department of Psychiatry and Behavioral Health, Ohio State University

[12]Department of Psychology, University of North Carolina at Chapel Hill

[13]Department of Psychiatry, Johns Hopkins University

Abstract

Corresponding author: Michele Bertocci, Postal Address: Western Psychiatric Institute and Clinic, Loeffler Building, room 203, 121 Meyran Avenue, Pittsburgh, PA 15213, bertoccima@upmc.edu.

*Bertocci and Bebko contributed equally as 1st authors

Disclosure statement:

Bertocci, Bebko, Olino, Fournier, Iyengar, Horwitz, Axelson, Holland, Schirda, Versace, Almeida, Perlman, Diwadkar, Travis, Bonar, Gill, and Forbes have no financial interests or potential conflicts of interest.

Behavioral and emotional dysregulation in childhood may be understood as prodromal to adult psychopathology. Additionally, there is a critical need to identify biomarkers reflecting underlying neuropathological processes that predict clinical/behavioral outcomes in youth. We aimed to identify such biomarkers in youth with behavioral and emotional dysregulation in the Longitudinal Assessment of Manic Symptoms (LAMS) study. We examined neuroimaging measures of function and white matter in the whole brain using 80 youth aged 14.0(sd=2.0) from 3 clinical sites. Linear regression using the LASSO method for variable selection was used to predict severity of future behavioral and emotional dysregulation [measured by the Parent General Behavior Inventory-10 Item Mania Scale (PGBI-10M)] at a mean of 14.2 months follow-up after neuroimaging assessment. Neuroimaging measures, together with near-scan PGBI-10M, a score of manic behaviors, depressive behaviors, and sex, explained 28% of the variance in follow-up PGBI-10M. Neuroimaging measures alone, after accounting for other identified predictors, explained approximately one-third of the explained variance, in follow-up PGBI-10M. Specifically, greater bilateral cingulum length predicted lower PGBI-10M at follow-up. Greater functional connectivity in parietal-subcortical reward circuitry predicted greater PGBI-10M at follow-up. For the first time, data suggest that multimodal neuroimaging measures of underlying neuropathologic processes account for over a third of the explained variance in clinical outcome in a large sample of behaviorally and emotionally dysregulated youth. This may be an important first step toward identifying neurobiological measures with the potential to act as novel targets for early detection and future therapeutic interventions.

Keywords

youth; behavioral and emotional dysregulation; prediction; fMRI; diffusion imaging

Introduction

Increasingly, neuroimaging studies are identifying biomarkers reflecting underlying neuropathologic processes that are predictive of clinical outcomes in adults.(1) Studies have shown, for example, that measures of neural structure and function can predict response to psychotherapy and psychotropic medications in adults with major depressive disorder (MDD) and anxiety disorders (AnxD). (2–4) In studies of youth with MDD, neural activity predicted response to CBT (5) as well as magnitude of depressive symptoms one to two years after neuroimaging assessment. (6, 7) In youth with AnxD, neural activity measured by fMRI (8) and Evoked Response Potentials (ERP) (9) predicted improvement in anxiety symptoms. Although still a nascent research field, the latter studies indicate feasibility of neuroimaging to identify measures of neural function reflecting underlying neuropathologic processes that, over and above clinical and demographic measures, predict future behavioral outcomes in youth with psychiatric disorders. Larger sample sizes, multimodal neuroimaging techniques, and sophisticated statistical analyses that allow testing of a large number of potential predictor variables are needed to fully examine the extent to which combinations of measures of neural structure and function along with clinical, demographic, genetic, and environmental factors predict future outcomes in youth. LASSO (Least Absolute Shrinkage and Selection Operator) regression is one such statistical technique that has been adopted for use in genetic studies (10–14) and is gaining favor in clinical research

including fMRI (15, 16). This technique allows for testing of a large number of potential predictor variables, relative to the number of study participants, while minimizing model error and minimizing the risk of overfitting.

The goal of the present study was to identify measures of neural function and structure predicting future behavioral and emotional dysregulation in a large group of youth in the Longitudinal Assessment of Manic Symptoms (LAMS) study. LAMS is an ongoing multi-site study examining longitudinal relationships among the course of symptoms, outcomes, and neural mechanisms associated with different clinical trajectories, in youth with symptoms characterized by behavioral and emotional dysregulation. (17, 18) It is ideally suited as a platform study in which to identify neuroimaging measures predicting future levels of behavioral and emotional dysregulation in youth.

A novel feature of LAMS is that it adopts both a conventional diagnostic (categorical) and a symptom (dimensional) approach to characterize severity of psychiatric symptoms and underlying neural mechanisms in youth. The latter approach supports the NIMH's Research Domain Criteria (RDoC) (19) and expectations, (20) aiming to elucidate neuropathologic processes associated with dimensions of psychopathology that cut across different diagnostic categories, which in turn may help identify neurobiological markers that predict future outcome. One dimensional measure of behavior employed in LAMS is the Parent General Behavior Inventory-10 Item Mania Scale (PGBI-10M), a parental report of behavioral and emotional dysregulation in youth that specifically captures behaviors associated with difficulty regulating mood and energy. (21, 22) In LAMS youth, PGBI-10M scores were elevated across multiple diagnostic categories (17, 18) and predicted clinical outcome. (23) Furthermore, we previously reported in LAMS youth relationships between functional and white matter structural abnormalities in neural circuitry supporting reward processing and emotional regulation with dimensional and categorical measures of affective pathology. (24, 25) This neural circuitry comprises prefrontal cortical, striatal, and insula regions (25) and white matter tracts connecting these prefrontal cortical and subcortical regions, including uncinate fasciculus, cingulum, and forceps minor. (26) Given the above cross-sectional associations among these neuroimaging measures, PGBI-10M, affective pathology, and outcome,(23) these neuroimaging measures are promising candidate neural predictors of future levels of behavioral and emotional dysregulation, and the present longitudinal study sought to test these predictive associations, 14.2 months later.

We hypothesized that in LAMS youth, future behavioral and emotional dysregulation, measured by follow-up PGBI-10M, would be predicted by: 1) neural function, measured by the magnitude of both activity and functional connectivity (FC), in prefrontal-cortical-striatal reward circuitry; and 2) diffusion imaging (DI) measures of white matter structure in tracts across the whole brain, but especially in the tracts supporting emotion processing noted above. Given that outcome has been consistently predicted by stability of psychopathology and by demographic factors such as age, (23, 27, 28) we also aimed to determine the relative proportion of future behavioral and emotional dysregulation predicted by neuroimaging, over and above clinical and demographic measures.

Methods

Participants

We recruited 130 youth (9–18 years; Table 1) with a variety of symptoms and diagnoses from three LAMS sites [Case Western Reserve University (n=32); Cincinnati Children's Hospital (n=48); University of Pittsburgh Medical Center (n=50)] to participate in the neuroimaging component of the LAMS second 5-year period (LAMS-2). Participants from the first 5-year period (LAMS-1) were selected to include approximately equal numbers from each site: 1) with high (≥12) versus low (<12) PGBI-10M scores; 2) who were older (≥13 years) versus younger (≤12 years) on scan day; 3) who were male versus female. Institutional Review Boards approved the study at each site. Parent/guardian consent and child assent were obtained.

Clinical Assessments

Assessments used in this analysis included parent/guardian's reported PGBI-10M, (21, 22) which has shown good reliability and diagnostic discrimination (21, 22) and the Depression Rating Scale (KDRS) (29) and Mania Rating Scale (KMRS) (30) supplements from the Schedule for Affective Disorders and Schizophrenia for School-Age Children, Present and Lifetime Version with supplemental questions from Washington University (K-SADS-PL-W), a well validated clinician interview with good psychometric properties. (29) Psychiatric diagnoses were confirmed by a licensed psychiatrist or psychologist and included bipolar spectrum disorder (BPSD), major depressive disorder (MDD), Anxiety disorder (AnxD), ADHD, and disruptive behavior disorder (DBD); frequency of diagnoses are reported in Table 1.

PGBI-10M scores were obtained on or near the day of scan (TIME1) and at follow-up interviews [(mean=14.2 months (range: 4.8–23.7)] after neuroimaging scans (TIME2). TIME1:PGBI-10M and TIME2:PGBI-10M scores differed significantly ($t(79) = 2.13$, $p = .036$) [TIME1:PGBI-10M: mean(SD) =5.96(5.95), TIME2:PGBI-10M= 4.59(5.2)] and were only moderately correlated r=.47.

Exclusion Criteria

Exclusion criteria were: systemic medical illnesses, neurological disorders, history of trauma with loss of consciousness, use of central nervous system effecting non-psychotropic medications, IQ<70 assessed by the Wechsler Abbreviated Scale of Intelligence (WASI), positive drug and/or alcohol screen on the day of MR scan, alcohol/substance abuse in the past 3 months (determined by the K-SADS-PL-W), significant visual disturbance, non-English speaker, autistic spectrum disorders/developmental delays, pregnancy, claustrophobia, and metal in the body. Participants were excluded for excessive head movement,(31) data acquisition artifact, incomplete data acquisition, and follow-up nonattendance (n=50), leaving 80 LAMS youth (Age=9.89–17.7). Excluded youth were younger, had lower IQ, were more likely to have a DBD, and had lower maternal education (Table 1).

Reward Task Description

Measures of reward-related neural activity were acquired using a validated, approximately six minute, block-design card guessing reward task. (31) For each guessing trial, participants guessed via button press whether the value of a card shown on the screen would be higher or lower than 5 (3000 msec) (possible value of 1 to 9, but whose value was not yet revealed). Next, the card's actual value was presented (500 msec) and outcome feedback was presented (Win: green upward-facing arrow; Loss: red downward-facing arrow, 500 msec). After each trial, a fixation cross was presented (3000 msec intertrial interval). Control trials consisted of participants pressing a button to the letter "X" (3000 msec). They then viewed an asterisk (500 msec), yellow circle (500 msec), and fixation cross (3000 msec intertrial interval).

The paradigm included 9 blocks: 3 win (80% win, 20% loss trials), 3 loss (80% loss, 20% win trials), and 3 control (constant in earnings) blocks. Control blocks had 6 control trials, while guessing blocks (Win and Loss) had 5 trials in an oddball format with preset outcome order (Win block: win, win, win, loss, win; Loss block: loss, loss, win, loss, loss). Participants practiced the task and practiced minimizing head movement in an fMRI simulator before scanning. Outcome probabilities were fixed, however the experimenter led participants to believe that performance determined outcomes. Participants were encouraged to both perform well and to stay as still as possible.

Neuroimaging Data Acquisition and Processing

fMRI data were collected on a 1) 3T Siemens Verio MRI scanner at CWRU, 2) 3T Philips Achieva X-series MRI scanner at CCH, and 3) 3T Siemens Trio MRI scanner at UPMC. An axial 3D magnetization prepared rapid gradient echo (MP-RAGE) sequence (192 axial slices 1 mm thick; flip angle=9°; field of view=256 mm × 192 mm; TR=2300 msec; TE=3.93 msec; matrix=256×192) acquired T1-weighted volumetric anatomical images covering the whole brain. A reverse interleaved gradient echo planar imaging (EPI) sequence (38 axial slices 3.1 mm thick; flip angle=90°; field of view=205 mm; TR=2000 msec; TE=28 msec; matrix=64×64) acquired T2-weighted BOLD images covering the whole cerebrum and most of the cerebellum.

Preprocessing involved realignment, coregistration, segmentation, normalization into a standard stereotactic space (Montreal Neurologic Institute, MNI; http://www.bic.mni.mcgill.ca), and spatially smoothing using a Gaussian kernel (FWHM: 8mm). The detailed preprocessing stream is described in supplemental materials. A two level random-effects procedure was then used to conduct whole brain analyses. At the first level individual whole brain statistical maps were constructed to evaluate the main condition contrasts of interest: win versus control. Movement parameters obtained from the realignment stage of preprocessing served as covariates of no interest.

Psychophysiological Interaction Methodology

Given the key role of the ventral striatum (VS) in reward processing, we used a VS (bilateral spheres ±9,9,-8; radius=8mm (32, 33)) seed region to examine FC between VS and reward-related wholebrain activity during the Win>Control contrast, using Psychophysiological Interaction (PPI) analysis. After processing the Reward task as above, we extracted

associated VS suprathreshold clusters as the seed region and created a PPI vector by multiplying the mean time series from the seed region by task condition vectors. Next, we ran single subject first level analyses for each task condition using 3 primary regressors: PPI vector, time course vector, and task condition vector were created, controlling for movement parameters.

Diffusion Imaging (DI) Methodology

DI data were collected in the same scanning session as fMRI data at the above three sites, and were processed using ExploreDTI, Freesurfer and Tracts Constrained by Underlying Anatomy (Tracula) software. (34) White matter tracts were automatically reconstructed using probabilistic tractography accounting for anatomy (see supplemental materials). DI analysis is sensitive to diffusivity of water in white matter tracts in the brain. In white matter tracts with axons that have densely packed collinear fibers, water diffuses along the principal/longitudinal axon but in non-collinear axons (crossing fibers), water moves along two or more directions. Measures include axial diffusivity; Lambda1 (L1; diffusivity along the principal axis); radial diffusivity (RD; diffusivity along directions perpendicular to the longitudinal axis); length and volume of tracts. Tracts with densely-packed collinear axons are characterized by high L1; tracts with non-collinear axons are characterized by high RD; while white matter damage is characterized by high RD. Measures of fractional anisotropy (FA) were not included, as these were not independent of L1 and RD measures for a given tract, as FA is computed as the ratio between L1 and RD.

Combining Data Across Sites

Merging neuroimaging data from multiple sites is feasible given the use of appropriate measures.(35, 36) To control for inter-site scanner variability and to combine neuroimaging data across our three sites we performed the following. First, we implemented global normalization to improve the degree to which first-level models met model assumptions at each site(37). Second, the Biomedical Informatics Research Network (BIRN; http://www.nbirn.net) standards for data acquisition and information sharing were implemented. Scanner signal-to-noise-ratio (SNR) was collected using a BIRN phantom and monitored for stability monthly at each scanner site (36, 38). Third, we used scanning site as a predictor variable in all relevant statistical models.

Neuroimaging IVs

1) Functional measures—Significant wholebrain mean BOLD activity to the Win>Control contrast was extracted (voxelwise p≤.001, clusterwise 3DClusterSim p≤.05 corrected; Table 2, minimum k=38) as recommended (39–43). Full weight half max (FWHM) x, y, and z smoothing parameters used in 3DClusterSim were acquired from the SPM 2nd level output. Similarly for PPI, significant whole brain parameter estimates were extracted from regions showing significant positive modulation of functional connectivity with the VS seed to the Win>Control contrast (voxelwise p≤0.05, clusterwise 3DClusterSim p≤0.05 corrected, minimum k=134) as in previous studies. (44–46) These mean activity and functional connectivity measures were included as predictor variables.

2) Structural measures—We chose two orthogonal measures of white matter structure: longitudinal diffusivity (L1), radial diffusivity (RD), plus volume, and length. These measures were extracted from all major tracts connecting prefrontal, parietal, temporal, and subcortical regions in the whole brain, including bilateral tracts of the anterior thalamic radiation, cingulate angular bundle, cingulum, inferior longitudinal fasciculus, parietal superior longitudinal fasciculus, temporal superior longitudinal fasciculus, uncinate fasciculus, forceps major and forceps minor. We additionally included the corticospinal tract as a control reference tract.

Data Analytic Plan

The TIME2:PGBI-10M was not distributed normally [range=0–23, mean=4.59 (5.2), median=3.0], and residuals calculated from initial Ordinary Least Squares models were likewise non-normal. Residuals appeared to follow a Poisson distribution; therefore, to model TIME2:PGBI-10M data we used methods assuming a Poisson distribution. Because we had data with more variables than observations, we used a LASSO regression analysis for data selection and reduction using the freely available GLMNET package in R(47). LASSO is a modified form of least squares regression that penalizes complex models with a regularization parameter (λ).(48) This penalization method shrinks coefficients toward zero, and eliminates unimportant terms entirely(47–49), thereby minimizing prediction error, reducing the chances of overfitting, and enforcing recommended sparsity in the solution(48).

GLMNET uses a quadratic approximation to the loglikelihood (an outer Newton loop) and then cyclical coordinate descent algorithm (50, 51) that is computed along a regularization path (an inner weighted least squares loop) to optimize the penalized loglikelihood; this is programmed in FORTRAN. Cyclical coordinate descent refers to optimization of each parameter separately, holding all others fixed until coefficients stabilize. Regularization is the process of adding constraints to a problem to avoid over fitting. Regularization in GLMNET for a Poisson regression is performed by producing the path of tuning parameters (λ) and solving the following equation over the range of λ, thereby identifying the optimal λ.

$$\min_{\beta_0\beta} -\frac{1}{N} l(\beta|X,Y)+\lambda\left((1-\alpha)\sum_{i=1}^{N}\beta_i^2/2+\alpha\sum_{i=1}^{N}|\beta_i|\right)$$

GLMNET uses cross validation to identify the optimal penalty term (λ) that would minimize the mean cross validated error for our model and guard against Type III errors (testing hypotheses already suggested by the data). We used a k=10 fold cross validation approach.

A test statistic or p-value for LASSO that has a simple and exact asymptotic null distribution was proposed by Lockhart(52), but has not yet been rigorously tested for conventional use or implemented in standard statistical packages. We thus report non-zero coefficients identified in the model, the rate ratio (exponentiated coefficients), and pseudo r-squared computed from Akaike Infromation Criteria (AIC) of standard leave-one-out Poisson regression model analyses. The leave-one-out procedure involves comparing the full model (all appropriate

predictor variables) with the model containing fewer predictor variables (removing the predictor variables of interest). The difference in these models is the explained variance of the left-out variables.

For our analysis, TIME2:PGBI-10M scores served as the outcome variable, and TIME1:PGBI-10M, in addition to other TIME1 clinical and demographic variables acquired on or near scan-day (TIME1), were predictor variables. TIME1 measures included the above BOLD, functional connectivity, and DI neuroimaging measures, TIME1:PGBI-10M, KMRS, KDRS scores, and diagnoses (ADHD, BPSD, MDD, DBD, AnxD), age, IQ, sex, medication status (taking versus not taking each psychotropic medication class: stimulant, non-stimulant ADHD, mood stabilizer, antipsychotic, and antidepressant psychotropic medications), scan site, and days between TIME1:PGBI-10M and TIME2:PGBI-10M.

Results

Seven predictors together optimized model fit using the minimum λ identified by cross validation. This minimum λ corresponds to the penalty at which minimal mean squared error (MSE) is achieved(47). Of these, three were clinical variables (TIME1:PGBI-10M, KMRS, and KDRS scores), one was sex, and three were neuroimaging variables (right and left cingulum length, and VS-right parietal connectivity. Table 3).

Exponentiated parameters indicated that greater values of right and left cingulum length predicted lower TIME2:PGBI-10M (i.e., better behavioral and emotional regulation). By contrast, greater VS-parietal functional connectivity, higher TIME1:PGBI-10M, being female, higher TIME1:KMRS, and TIME1:KDRS predicted higher TIME2:PGBI-10M scores (i.e., worse behavioral and emotional dysregulation).

A pseudo r-squared of .28 was calculated for the standard Poisson model containing seven non-zero predictors identified from the LASSO regression model versus an intercept only model, indicating that 28% of the TIME2:PGBI-10M variance was explained by the model. Leave-one-out analysis showed that three neuroimaging variables (right and left cingulum length and VS-right parietal functional connectivity) explained 10% of the TIME2:PGBI-10M variance, and four clinical and demographic variables (TIME1:PGBI-10M, TIME1:KMRS, TIME1:KDRS, and sex) explained 15% of the TIME2:PGBI-10M variance.

Discussion

Our goal was to assess the ability of multimodal neuroimaging measures to predict future levels of behavioral and emotional dysregulation in psychiatrically-unwell youth. We used a LASSO regression model, along with cross-validation, an approach that penalizes complex models with a regularization parameter and identifies the parameter that minimizes the mean squared error, sending unimportant coefficients to zero. Findings indicated that 28% of the variance in a key measure of behavioral and emotional dysregulation, PGBI-10M score, measured at a mean of 14.2 months after neuroimaging assessment was predicted by bilateral cingulum length and VS-right parietal functional connectivity, together with TIME1:PGBI-10M score, TIME1:KMRS score, TIME1:KDRS score, and sex. Our

conservative analytic approach revealed that neuroimaging measures alone, even after accounting for other significant predictors, predicted 10% of the variance, ie., approximately one-third of the explained variance, in this outcome measure.

We show here that greater FC between VS and parietal cortex, components of neural circuitry supporting reward processing, (53–56) predicted worse future behavioral and emotional dysregulation. Greater activity in this VS-parietal neural circuitry to reward cues and outcomes has been reported in individuals with substance use disorders, and greater severity of behavioral and emotional dysregulation.(53, 55) These findings suggest that neuroimaging measures of a key underlying neuropathologic process in bipolar disorder, heightened reward sensitivity,(57) may predict worse future behavioral and emotional dysregulation in psychiatrically-unwell youth. Our findings further indicate that the magnitude of functional connections among different reward circuitry regions, reflecting more global measures of functioning in this circuitry, rather than activity within specific regions of this circuitry, contribute to future outcome.

By contrast, better future behavioral and emotional regulation was predicted by greater bilateral cingulum length. Most DI studies of adults and youth with BPSD or subthreshold symptoms reported altered FA and RD in key WM tracts implicated in emotion regulation, including the cingulum. (58, 59) Our findings are the first to our knowledge, however, to suggest that greater cingulum length may be associated with capacity for better future behavioral and emotional regulation in youth. Given that the cingulum has projections within subcortical regions and sends long association projections between prefrontal cortex and other cortical areas,(60) including, along with the superior longitudinal fasciculus, connections to key prefrontal and parietal cortical regions implicated in attentional control, (61, 62) longer cingulum tract length may increase capacity for attentional control that, in turn, may confer protection against future worsening of behavioral and emotional dysregulation.

Non-neuroimaging measures also predicted future behavioral and emotional dysregulation. Greater TIME1:PGBI-10M predicted worse future behavioral and emotional dysregulation. Given that this is a repeated measure, this is likely an indication of the measure's consistency over time. It was thus necessary to adjust for the baseline score to clarify effects of other predictor variables. Additionally, TIME1:KMRS and TIME1:KDRS scores predicted worse future behavior and emotional dysregulation. These scores, although not highly correlated with TIME1:PGBI-10M ($r<.48$ and .19 respectively), are measures of mood dysregulation, and would thus also be likely to predict future mood dysregulation, as measured by TIME2:PGBI-10M. They also incorporate the youth's perspective and clinical observations of youth behavior, in addition to the parent perspective captured in the PGBI-10M. Finally, sex showed a non-zero coefficient in the LASSO model, with being female associated with worse future behavioral and emotional regulation, consistent with the well-established increase in risk for depression among females in adolescence and early adulthood.

Diagnoses did not predict TIME2:PGBI-10M, suggesting that, in support of the RDoC approach, measures of symptom dimensions, rather than diagnostic categories, may better

reflect underlying neuropathologic processes in psychiatric illness. This was despite the use of standardization in the LASSO regression model, which assigns the same scale to all variables, thereby consistently penalizing each variable(63). Overall, our findings are aligned with one of the few neuroimaging predictor studies in youth (10–16 years) with anxiety disorders,(8) in which 36% of variance in outcome Clinical Global Impressions-Severity (CGI-S) score, was predicted using a combination of near-scan:CGI-S and left amygdala activity. This amount of explained outcome variance in this study was similar to that predicted by the combination of neuroimaging and clinical measures in the present study. The explained variance in outcome predicted by neuroimaging alone was not reported in this previous study, however.

There were limitations. We focused on whole brain reward neural circuitry and white matter tracts. Including other neuroimaging measures, such as gray matter volumes or cortical thickness, may improve future outcome predictions. (We report findings in supplemental materials from an additional LASSO model that included measures of cortical thickness, along with the neuroimaging, clinical and demographic measures included in the present LASSO model, as predictors). We assumed a linear model with a Poisson distribution due to evidence of linear growth in white matter volume among youth in this age group (64). Nonlinear models may also be considered in future studies. We used standard PPI in our analyses, as in previous studies in youth(65). Other methods of functional connectivity analyses may yield different findings. In addition, while other outcome measures could have been included, the PGBI-10M is the key LAMS-2 measure of behavioral and emotional dysregulation, and, as such, was the preferred outcome measure. Additionally, the contribution of pubertal development could not be considered as it was not measured during TIME1 assessments. Many of the LAMS youth were medicated, although no class of psychotropic medication was a non-zero predictor of future TIME2:PGBI-10M. Finally, there has been recent debate about inflation of predictions in neuroimaging studies in individuals with psychiatric disorders.(66) We used a well-validated approach that penalizes complex models using regularization, cross validation, and enforces sparsity in model fit. As in any study, magnitudes of parameter estimates that we observed for each predictor need to be examined and refined in future replications and meta-analyses.

This is the first study, to our knowledge, to use a multimodal neuroimaging approach to predict future behavioral and emotional dysregulation in youth. Specifically, we show that after accounting for prior severity of behavioral and emotional dysregulation, approximately one-third of the explained variance of the severity of these symptoms in the future was predicted by a combination of neuroimaging measures of reward circuitry function and white matter structure in tracts in the whole brain. This study demonstrates for the first time that neuroimaging measures reflecting underlying neuropathological processes are significant predictors of a substantial proportion of variance in future behavioral and emotional dysregulation in youth. This is an important step toward identifying neurobiological measures characterizing youth at greatest risk of poor outcome, and provides promising neural targets for future therapeutic interventions.

Supplementary Material

Refer to Web version on PubMed Central for supplementary material.

Acknowledgements

Supported by the National Institute of Mental Health grants 2R01 MH73953 (Dr. Boris Birmaher and Dr. Mary L. Phillips, University of Pittsburgh), 2R01 MH73816 (Dr. Scott Holland, Children's Hospital Medical Center), 2R01 MH73967 (Dr. Robert Findling, Case Western Reserve University), and 2R01 MH73801(Dr. Mary Fristad, Ohio State University). The funding agency was not involved in the design and conduct of the study, the collection, management, analysis, or interpretation of the data, or the preparation, review, or approval of the manuscript. We would like to acknowledge Richard White, Gary Ciuffetelli, Eric Rodriguez, and Christine Demeter for their contributions to the study.

Dr. Findling receives or has received research support, acted as a consultant and/or served on a speaker's bureau for Alexza Pharmaceuticals, American Academy of Child & Adolescent Psychiatry, American Physician Institute, American Psychiatric Press, AstraZeneca, Bracket, Bristol-Myers Squibb, Clinsys, CogCubed, Cognition Group, Coronado Biosciences, Dana Foundation, Forest, GlaxoSmithKline, Guilford Press, Johns Hopkins University Press, Johnson & Johnson, KemPharm, Lilly, Lundbeck, Merck, NIH, Novartis, Noven, Otsuka, Oxford University Press, Pfizer, Physicians Postgraduate Press, Rhodes Pharmaceuticals, Roche, Sage, Seaside Pharmaceuticals, Shire, Stanley Medical Research Institute, Sunovion, Supernus Pharmaceuticals, Transcept Pharmaceuticals, Validus, and WebMD..

Dr. Frazier has received federal funding or research support from, acted as a consultant to, received travel support from, and/or received a speaker's honorarium from the Simons Foundation, Ingalls Foundation, Forest Laboratories, Ecoeos, IntegraGen, Kugona LLC, Shire Development, Bristol-Myers Squibb, National Institutes of Health, and the Brain and Behavior Research Foundation.

Dr. Arnold has had research funding from Curemark, Forest, Lilly, and Shire, advisory board honoraria from Biomarin, Novartis, Noven, Otsuka, Roche, Seaside Therapeutics, & Shire, consulting with Tris Pharma, and travel support from Noven. Dr. Youngstrom has consulted with Pearson, Lundbeck and Otsuka about assessment, as well as having grant support from the NIH.

Dr. Fristad receives royalties from Guilford Press, Inc., APPI, CFPSI and is a consultant to Physicians Postgraduate Press.

Dr. Birmaher receives royalties from for publications from Random House, Inc (New hope for children and teens with bipolar disorder) and Lippincott Williams & Wilkins (Treating Child and Adolescent Depression). He is employed by the University of Pittsburgh and the University of Pittsburgh Medical Center and receives research funding from NIMH.

Dr. Kowatch is a consultant for Forest Pharmaceutical, Astra-Zeneca and the REACH Foundation. He receives research support from NIMH. He is employed by Ohio State University and an editor for Current Psychiatry. Dr. Sunshine receives research support from Siemens Healthcare.

Dr Phillips is a consultant for Roche Pharmaceuticals.

References

1. Berkman ET, Falk EB. Beyond Brain Mapping Using Neural Measures to Predict Real-World Outcomes. Current Directions in Psychological Science. 2013; 22(1):45–50. [PubMed: 24478540]
2. Pizzagalli DA. Frontocingulate dysfunction in depression: toward biomarkers of treatment response. Neuropsychopharmacology. 2010; 36(1):183–206. [PubMed: 20861828]
3. Fu CH, Steiner H, Costafreda SG. Predictive neural biomarkers of clinical response in depression: a meta-analysis of functional and structural neuroimaging studies of pharmacological and psychological therapies. Neurobiology of Disease. 2013; 52:75–83. [PubMed: 22659303]
4. Shin LM, Davis FC, VanElzakker MB, Dahlgren MK, Dubois SJ. Neuroimaging predictors of treatment response in anxiety disorders. Biology of mood & anxiety disorders. 2013; 3(1):15. [PubMed: 23915782]

5. Forbes EE, Olino TM, Ryan ND, Birmaher B, Axelson D, Moyles DL, et al. Reward-related brain function as a predictor of treatment response in adolescents with major depressive disorder. Cogn Affect Behav Neurosci. 2010; 10(1):107–118. [PubMed: 20233959]
6. Masten CL, Eisenberger NI, Borofsky LA, McNealy K, Pfeifer JH, Dapretto M. Subgenual anterior cingulate responses to peer rejection: a marker of adolescents' risk for depression. Dev Psychopathol. 2011; 23(1):283–292. [PubMed: 21262054]
7. Morgan JK, Olino TM, McMakin DL, Ryan ND, Forbes EE. Neural response to reward as a predictor of increases in depressive symptoms in adolescence. Neurobiology of Disease. 2013; 52(0):66–74. [PubMed: 22521464]
8. McClure EB, Adler A, Monk CS, Cameron J, Smith S, Nelson EE, et al. fMRI predictors of treatment outcome in pediatric anxiety disorders. Psychopharmacology. 2007; 191(1):97–105. [PubMed: 16972100]
9. Hum KM, Manassis K, Lewis MD. Neurophysiological Markers That Predict and Track Treatment Outcomes in Childhood Anxiety. Journal of abnormal child psychology. 2013:1–13. [PubMed: 22773360]
10. Kohannim O, Hibar DP, Jahanshad N, Stein JL, Hua X, Toga AW, et al. Predicting Temporal Lobe Volume on Mri from Genotypes Using L(1)–L(2) Regularized Regression. Proc IEEE Int Symp Biomed Imaging. 2012:1160–1163. [PubMed: 22903144]
11. Wang Z, Xu W, Liu Y. Integrating full spectrum of sequence features into predicting functional microRNA-mRNA interactions. Bioinformatics. 2015; 30
12. Zemmour C, Bertucci F, Finetti P, Chetrit B, Birnbaum D, Filleron T, et al. Prediction of early breast cancer metastasis from DNA microarray data using high-dimensional cox regression models. Cancer Inform. 2015; 14(Suppl 2):129–138. [PubMed: 25983547]
13. Kohannim O, Hibar DP, Stein JL, Jahanshad N, Hua X, Rajagopalan P, et al. Discovery and Replication of Gene Influences on Brain Structure Using LASSO Regression. Front Neurosci. 2012; 6(115)
14. Luo Y, McShan D, Kong F, Schipper M, Haken RT. TH-AB-304-07: A Two-Stage Signature-Based Data Fusion Mechanism to Predict Radiation Pneumonitis in Patients with Non-Small-Cell Lung Cancer (NSCLC). Med Phys. 2015; 42(6):4926122.
15. Christensen JA, Zoetmulder M, Koch H, Frandsen R, Arvastson L, Christensen SR, et al. Data-driven modeling of sleep EEG and EOG reveals characteristics indicative of pre-Parkinson's and Parkinson's disease. J Neurosci Methods. 2014; 235:262–276. [PubMed: 25088694]
16. Yan S, Tsurumi A, Que YA, Ryan CM, Bandyopadhaya A, Morgan AA, et al. Prediction of multiple infections after severe burn trauma: a prospective cohort study. Ann Surg. 2015; 261(4): 781–792. [PubMed: 24950278]
17. Findling RL, Youngstrom EA, Fristad MA, Birmaher B, Kowatch RA, Arnold LE, et al. Characteristics of children with elevated symptoms of mania: the Longitudinal Assessment of Manic Symptoms (LAMS) study. The Journal of clinical psychiatry. 2010; 71(12):1664. [PubMed: 21034685]
18. Horwitz SM, Demeter C, Pagano ME, Youngstrom EA, Fristad MA, Arnold LE, et al. Longitudinal Assessment of Manic Symptoms (LAMS) Study: background, design and initial screening results. The Journal of clinical psychiatry. 2010; 71(11):1511. [PubMed: 21034684]
19. Insel T, Cuthbert B, Garvey M, Heinssen R, Pine D, Quinn K, et al. Research domain criteria (RDoC): toward a new classification framework for research on mental disorders. American Journal of Psychiatry. 2010; 167(7):748–751. [PubMed: 20595427]
20. Insel TR, Gogtay N. National institute of mental health clinical trials: New opportunities, new expectations. JAMA Psychiatry. 2014; 71(7):745–746. [PubMed: 24806613]
21. Youngstrom E, Meyers O, Demeter C, Youngstrom J, Morello L, Piiparinen R, et al. Comparing diagnostic checklists for pediatric bipolar disorder in academic and community mental health settings. Bipolar Disorders. 2005; 7(6):507–517. [PubMed: 16403176]
22. Youngstrom EA, Frazier TW, Demeter C, Calabrese JR, Findling RL. Developing a Ten Item Mania Scale from the Parent General Behavior Inventory for Children and Adolescents. The Journal of clinical psychiatry. 2008; 69(5):831. [PubMed: 18452343]

23. Frazier TW, Youngstrom EA, Horwitz SM, Demeter CA, Fristad MA, Arnold LE, et al. The Relationship of Persistent Manic Symptoms to the Diagnosis of Pediatric Bipolar Disorder. The Journal of clinical psychiatry. 2011; 72(6):846. [PubMed: 21457674]
24. Versace A, Acuff H, Bertocci MA, Bebko G, Almeida JR, Perlman SB, et al. White matter structure in youth with behavioral and emotional dysregulation disorders: a probabilistic tractographic study. JAMA Psychiatry. 2015; 72(4):367–376. [PubMed: 25715064]
25. Bebko G, Bertocci MA, Fournier JC, Hinze AK, Bonar L, Almeida JR, et al. Parsing Dimensional vs Diagnostic Category-Related Patterns of Reward Circuitry Function in Behaviorally and Emotionally Dysregulated Youth in the Longitudinal Assessment of Manic Symptoms Study. JAMA Psychiatry. 2013; 71(1):71–80. [PubMed: 24285346]
26. Versace A, Andreazza AC, Young LT, Fournier JC, Almeida JR, Stiffler RS, et al. Elevated serum measures of lipid peroxidation and abnormal prefrontal white matter in euthymic bipolar adults: toward peripheral biomarkers of bipolar disorder. Mol Psychiatry. 2014; 19(2):200–208. [PubMed: 23358158]
27. Loeber R, Green SM, Keenan K, Lahey BB. Which Boys Will Fare Worse? Early Predictors of the Onset of Conduct Disorder in a Six-Year Longitudinal Study. Journal of the American Academy of Child and Adolescent Psychiatry. 1995; 34(4):499–509. [PubMed: 7751264]
28. Leibenluft E, Cohen P, Gorrindo T, Brook JS, Pine DS. Chronic versus episodic irritability in youth: a community-based, longitudinal study of clinical and diagnostic associations. J Child Adolesc Psychopharmacol. 2006; 16(4):456–466. [PubMed: 16958570]
29. Kaufman J, Birmaher B, Brent DA, Rao U, Flynn C, Moreci P, et al. Schedule for Affective Disorders and Schizophrenia for School-Age Children-Present and Lifetime Version (K-SADS-PL): initial reliability and validity data. Journal of the American Academy of Child & Adolescent Psychiatry. 1997; 36(7):980–988. [PubMed: 9204677]
30. Axelson DA, Birmaher B, Brent DA, Wassick S, Hoover C, Bridge J, et al. A preliminary study of the Kiddie Schedule for Affective Disorders and Schizophrenia for School-Age Children mania rating scale for children and adolescents. Journal of child and adolescent psychopharmacology. 2003; 13(4):463–470. [PubMed: 14977459]
31. Forbes EE, Hariri AR, Martin SL, Silk JS, Moyles DL, Fisher PM, et al. Altered striatal activation predicting real-world positive affect in adolescent major depressive disorder. American Journal of Psychiatry. 2009; 166(1):64. [PubMed: 19047324]
32. Di Martino A, Scheres A, Margulies D, Kelly A, Uddin L, Shehzad Z, et al. Functional connectivity of human striatum: a resting state FMRI study. Cerebral Cortex. 2008; 18(12):2735–2747. [PubMed: 18400794]
33. Postuma RB, Dagher A. Basal ganglia functional connectivity based on a meta-analysis of 126 positron emission tomography and functional magnetic resonance imaging publications. Cerebral Cortex. 2006; 16(10):1508–1521. [PubMed: 16373457]
34. Yendiki A, Panneck P, Srinivasan P, Stevens A, Zöllei L, Augustinack J, et al. Automated probabilistic reconstruction of white-matter pathways in health and disease using an atlas of the underlying anatomy. Frontiers in Neuroinformatics. 2011; 5
35. Segall JM, Turner JA, van Erp TG, White T, Bockholt HJ, Gollub RL, et al. Voxel-based morphometric multisite collaborative study on schizophrenia. Schizophrenia Bulletin. 2009; 35(1): 82–95. [PubMed: 18997157]
36. Magnotta VA, Friedman L. Measurement of Signal-to-Noise and Contrast-to-Noise in the fBIRN Multicenter Imaging Study. Journal of Digital Imaging. 2006; 19(2):140–147. [PubMed: 16598643]
37. Eklund A, Andersson M, Josephson C, Johannesson M, Knutsson H. Does parametric fMRI analysis with SPM yield valid results? An empirical study of 1484 rest datasets. NeuroImage. 2012; 61(3):565–578. [PubMed: 22507229]
38. Friedman L, Glover GH, The FC. Reducing interscanner variability of activation in a multicenter fMRI study: Controlling for signal-to-fluctuation-noise-ratio (SFNR) differences. NeuroImage. 2006; 33(2):471–481. [PubMed: 16952468]
39. Pujol J, Soriano-Mas C, Alonso P, et al. MApping structural brain alterations in obsessive-compulsive disorder. Archives of General Psychiatry. 2004; 61(7):720–730. [PubMed: 15237084]

40. Goldin PR, Manber-Ball T, Werner K, Heimberg R, Gross JJ. Neural Mechanisms of Cognitive Reappraisal of Negative Self-Beliefs in Social Anxiety Disorder. Biological Psychiatry. 2009; 66(12):1091–1099. [PubMed: 19717138]
41. Surguladze S, Brammer MJ, Keedwell P, Giampietro V, Young AW, Travis MJ, et al. A differential pattern of neural response toward sad versus happy facial expressions in major depressive disorder. Biological Psychiatry. 2005; 57(3):201–209. [PubMed: 15691520]
42. Lynn M, Demanet J, Krebs R, Van Dessel P, Brass M. Voluntary inhibition of pain avoidance behavior: an fMRI study. Brain Struct Funct. 2014:1–12.
43. Woo C-W, Krishnan A, Wager TD. Cluster-extent based thresholding in fMRI analyses: Pitfalls and recommendations. NeuroImage. 2014; 91:412–419. [PubMed: 24412399]
44. Reeck C, Egner T. Emotional task management: neural correlates of switching between affective and non-affective task-sets. Social Cognitive and Affective Neuroscience. 2014
45. Somerville LH, Jones RM, Ruberry EJ, Dyke JP, Glover G, Casey BJ. The Medial Prefrontal Cortex and the Emergence of Self-Conscious Emotion in Adolescence. Psychological Science. 2013; 24(8):1554–1562. [PubMed: 23804962]
46. Ladouceur CD, Farchione T, Diwadkar V, Pruitt P, Radwan J, Axelson DA, et al. Differential Patterns of Abnormal Activity and Connectivity in the Amygdala–Prefrontal Circuitry in Bipolar-I and Bipolar-NOS Youth. Journal of the American Academy of Child & Adolescent Psychiatry. 2011; 50(12):1275.e2–1289.e2. [PubMed: 22115148]
47. Friedman J, Hastie T, Simon N, Tibshirani R. GLMNET. 2.0-2 ed. 2014
48. Tibshirani R. Regression Shrinkage and Selection via the Lasso. Journal of the Royal Statistical Society Series B (Methodological). 1996; 58(1):267–288.
49. Friedman J, Hastie T, Tibshirani R. Regularization Paths for Generalized Linear Models via Coordinate Descent. J Stat Softw. 2010; 33(1):1–22. [PubMed: 20808728]
50. Revolutionary Analytics. Trevor hastie presents glmnet: lasso and elastic-net regularization in R. 2013
51. Wu TT, Lange K. Coordinate decent algorithms for lasso penalized regression. The Annals of Applied Statistics. 2008; 2(1):224–244.
52. Lockhart R, Taylor J, Tibshirani RJ, Tibshirani R. A significance test for the lasso. 2014; (2):413–468.
53. Peters J, Büchel C. The neural mechanisms of inter-temporal decision-making: understanding variability. Trends in Cognitive Sciences. 2011; 15(5):227–239. [PubMed: 21497544]
54. Chen MY, Jimura K, White CN, Maddox WT, Poldrack RA. Multiple brain networks contribute to the acquisition of bias in perceptual decision-making. Front Neurosci. 2015; 9(63)
55. Boettiger CA, Mitchell JM, Tavares VC, Robertson M, Joslyn G, D'Esposito M, et al. Immediate reward bias in humans: fronto-parietal networks and a role for the catechol-O-methyltransferase 158(Val/Val) genotype. J Neurosci. 2007; 27(52):14383–14391. [PubMed: 18160646]
56. Jarbo K, Verstynen TD. Converging structural and functional connectivity of orbitofrontal, dorsolateral prefrontal, and posterior parietal cortex in the human striatum. J Neurosci. 2015; 35(9):3865–3878. [PubMed: 25740516]
57. Urosevic S, Abramson LY, Alloy LB, Nusslock R, Harmon-Jones E, Bender R, et al. Increased rates of events that activate or deactivate the behavioral approach system, but not events related to goal attainment, in bipolar spectrum disorders. J Abnorm Psychol. 2010; 119(3):610–615. [PubMed: 20677850]
58. Phillips ML, Swartz HA. A critical appraisal of neuroimaging studies of bipolar disorder: toward a new conceptualization of underlying neural circuitry and a road map for future research. Am J Psychiatry. 2014; 171(8):829–843. [PubMed: 24626773]
59. Paillere Martinot ML, Lemaitre H, Artiges E, Miranda R, Goodman R, Penttila J, et al. White-matter microstructure and gray-matter volumes in adolescents with subthreshold bipolar symptoms. Mol Psychiatry. 2014; 19(4):462–470. [PubMed: 23628983]
60. Schmahmann, JD.; Pandya, DN. Fiber Pathways of the Brain. Cary, NC, USA: Oxford University Press, USA; 2009.

61. Heilbronner SR, Haber SN. Frontal cortical and subcortical projections provide a basis for segmenting the cingulum bundle: implications for neuroimaging and psychiatric disorders. J Neurosci. 2014; 34(30):10041–10054. [PubMed: 25057206]

62. Mufson EJ, Pandya DN. Some observations on the course and composition of the cingulum bundle in the rhesus monkey. J Comp Neurol. 1984; 225(1):31–43. [PubMed: 6725639]

63. Tibshirani R. The lasso method for variable selection in the cox model. Statistics in medicine. 1997; 16:385–395. [PubMed: 9044528]

64. Brain Development Cooperative Group. Total and Regional Brain Volumes in a Population-Based Normative Sample from 4 to 18 Years: The NIH MRI Study of Normal Brain Development. Cerebral Cortex. 2012; 22(1):1–12. [PubMed: 21613470]

65. Singh MK, Kelley RG, Howe ME, Reiss AL, Gotlib IH, Chang KD. Reward processing in healthy offspring of parents with bipolar disorder. JAMA Psychiatry. 2014; 71(10):1148–1156. [PubMed: 25142103]

66. Whelan R, Garavan H. When Optimism Hurts: Inflated Predictions in Psychiatric Neuroimaging. Biol Psychiatry. 2013; 15(13) 00457-5.

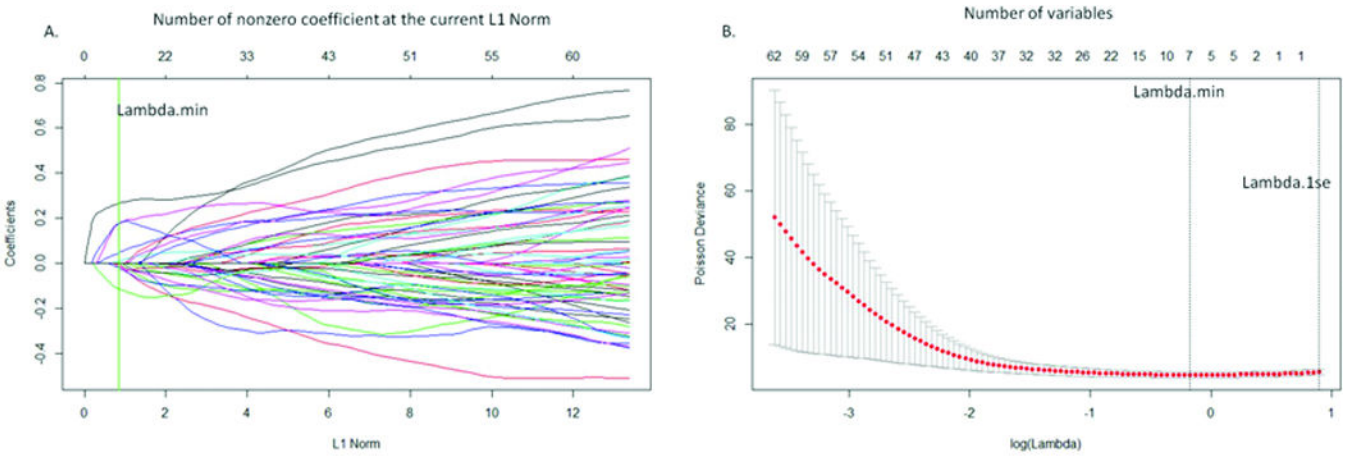

Figure 1. LASSO plots generated in GLMNET

A. Plot of variable fit. Each curve corresponds to an independent variable in the full model prior to optimization. Curves indicate the path of each variable coefficient as λ varies. Lambda.min corresponds to the λ which minimizes mean squared error in the model and was used for the selection of the seven predictor variables B. Plot of non-zero variable fit after cross validation. Representation of the 10-fold cross validation performed in LASSO that chooses the optimal λ. Lambda.min corresponds to the λ which minimizes mean squared error and was used for variable selection. Lambda.1se corresponds to the λ that is one standard error from the lambda.min.

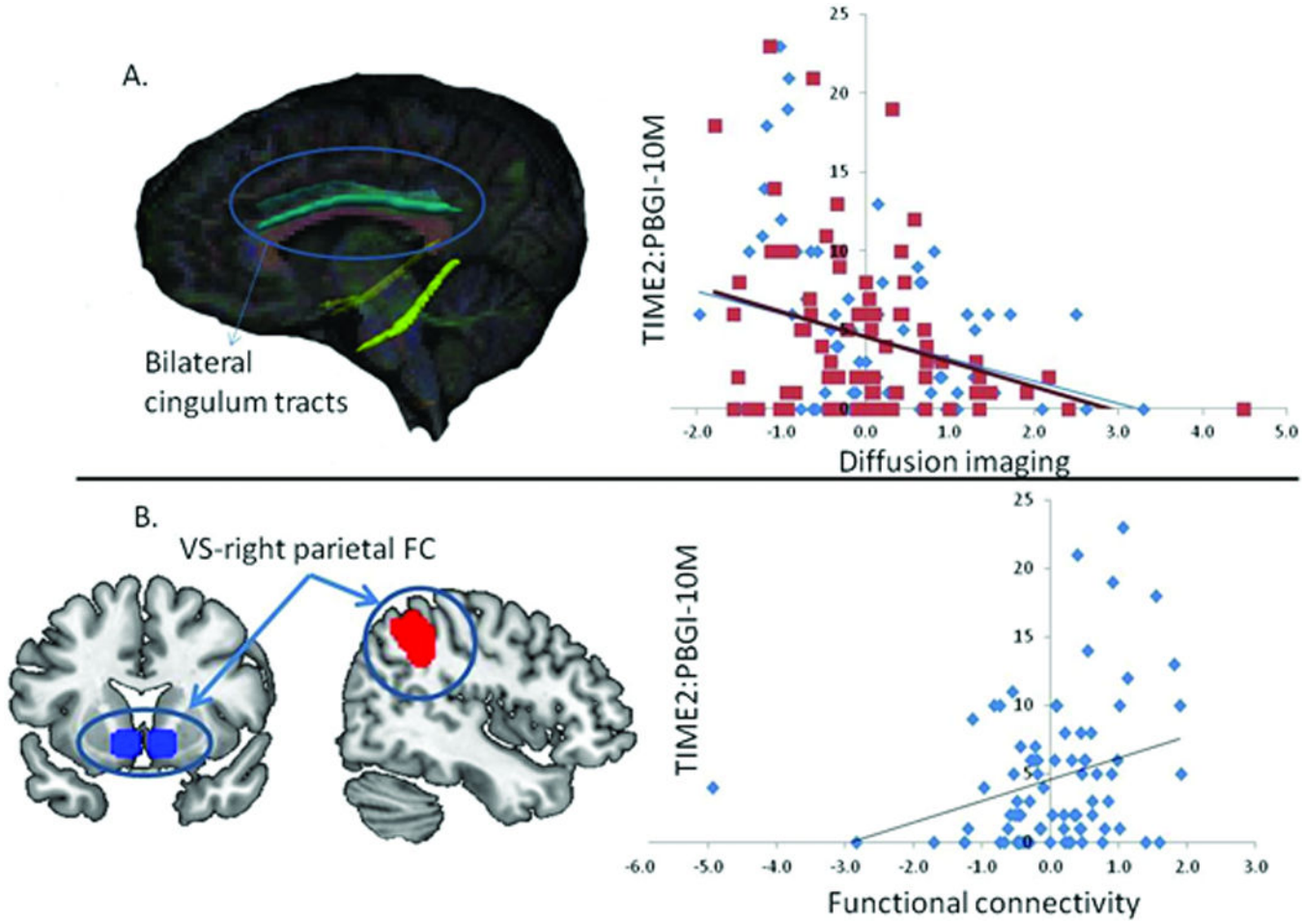

Figure 2. Representation of neural variables showing nonzero relationships with TIME2:PGBI-10M after LASSO regression and scatter plots of the linear relationships of these variables

All statistical analyses assumed an underlying Poisson distribution. A. Representation of bilateral cingulum tracts in a standard brain. Blue diamonds and trend line represent the relationship between left cingulum length and TIME2:PGBI-10M scores. Red squares and trend line represent the relationship between right cingulum length and TIME2:PGBI-10M scores. B. Representation of ventral striatum- right parietal functional connectivity (right parietal target region: mni: 48, −46, 52, k=314) in a standard brain. Scatter plot and trend line represent the relationship between vs-right parietal functional connectivity and TIME2:PGBI-10M scores.

Table 1

Comparison of participants used in the analyses (n=80) and those who were removed due to movement, incomplete fMRI/DTI acquisition, or incomplete follow-up data (n=50).

	Participants included in data analysis n=80	Participants not included in data analysis n=50	Statistic	p
Demographic Information				
Age	14.0(2)	12.82(1.9)	$t_{(128)} = -3.32$	.001
Sex (females)	33	15	χ^2=1.67	.196
IQ	104.38(17.02)	94.46(13.22)	$t_{(121.9)} = -3.72$	<.001
SES (primary caregiver education)			χ^2= 9.54	.049
No/some HS	3	5		
HS Diploma	16	19		
Some post HS	19	10		
Associate's Degree	23	11		
Bachelor's Degree or higher	19	5		
Clinical Measures				
Semi-annual assessment closest to scan				
PGBIM10	6.04(5.95)	6.47(6.60)	$t_{(126)} = .38$	.705
Scan day assessments				
KDRS	4.13(4.8)	3.40(4.5)	$t_{(126)} = -.85$	.395
KMRS	4.60(7.0)	4.10(6.4)	$t_{(126)} = -.40$	.690
SCARED	10.63(10.2)	13.18(13.2)	$t_{(83.0)} = 1.16$	.251
Diagnosis				
Major Depressive Disorder	23	15	χ^2= .023	.879
Bipolar spectrum disorder	30	13	χ^2=1.84	.175
ADHD	61	43	χ^2= 1.84	.176
Anxiety Disorder	28	11	χ^2= 2.48	.116
Disruptive Behavior Disorder	47	38	χ^2=4.05	.044
Psychotropic medication use	48	27	χ^2= .45	.501
Site			χ^2=3.20	.202
University of Pittsburgh Medical Center	26	24		
Case Western Reserve University	21	11		
Cincinnati Children's Hospital	33	15		

Parental General Behavior Inventory-10 Item Mania scale (PGBI-10M), Screen for Child Anxiety Related Emotional Disorders(SCARED), Schedule for Affective Disorders and Schizophrenia for School-Age Children Mania Rating Scale(KMRS), and Schedule for Affective Disorders and Schizophrenia for School-Age Children Depression Rating Scale(KDRS). Data are mean (SD) for age, IQ, and clinical measures. For all other variables data are total n. P-values are = unless specified.

Mol Psychiatry. Author manuscript; available in PMC 2016 August 23.

Table 2

Reward-related neural activity and functional connectivity in LAMS youth at Time 1.

			MNI Coordinates			Statistic	
Region	**BA**	**k**	**x**	**y**	**z**	**Test Statistic (df)**	$p_{uncorrected}$
Win>control Activity							
Right parietal cortex	40	399	48	−52	43	t(79)=6.24	<0.001
Left parietal cortex	40	443	−39	−58	46	t(79)=5.95	<0.001
Right prefrontal cortex	8	532	6	32	46	t(79)=6.00	<0.001
Corpus Callosum		125	6	−25	25	t(79)=5.46	<0.001
Right Insula		186	30	23	−5	t(79)=5.99	<0.001
Left motor cortex	6	372	−39	5	49	t(79)=5.60	<0.001
Right middle temporal gyrus	21	105	60	−31	−11	t(79)=5.03	<0.001
Right DLPFC	9	419	45	32	31	t(79)=4.89	<0.001
Left mPFC	10	234	−36	50	16	t(79)=5.34	<0.001
Left inferior frontal gyrus	45	180	−48	17	4	t(79)=5.03	<0.001
Right Primary visual area	17	39	12	−76	10	t(79)=3.93	<0.001
Left caudate		52	−9	8	4	t(79)=3.91	<0.001
Win>control Connectivity							
Right parietal cortex	40	314	48	−46	52	t(79)=4.59	<0.001
Left parietal cortex	7	365	−36	−52	55	t(79)=4.06	<0.001
Right middle frontal gyrus	9	289	42	38	22	t(79)=3.64	<0.001
Right prefrontal cortex	8	185	3	26	58	t(79)=3.17	<0.001

Win>Control Activity resulted from whole-brain analyses using voxelwise p<.001 and p<.05, 3DClusterSim corrected. Win>Control functional connectivity resulted from whole brain analyses using a bilateral ventral striatum seed region, voxelwise p<.05 and p<.05, 3DClusterSim corrected. Each row in the table represents the peak voxel within the specified region.

Abbreviations: BA = Brodmann area; df=degrees of freedom; k = cluster size in voxels; MNI=Montreal Neurological Institute coordinates; $p_{uncorrected}$=uncorrected voxelwise *p* value; t=t-test statistical value; DLPFC=dorsolateral prefrontal cortex.

Table 3

Nonzero coefficients generated from GLMNET using a LASSO regression with Poisson family model.

Variable	LASSO derived Coefficient	Exponentiated coefficient	Percent deviance explained by the addition of variable to model
TIME1:PGBI-10M	0.255	1.29	.136
VS-right parietal functional connectivity	0.153	1.17	.082
Left cingulum length	−0.097	0.91	.061
Sex	0.146	1.16	.024
KMRS	0.034	1.03	.008
Right cingulum length	−0.008	0.99	.005
KDRS	0.001	1.00	.002

Exponentiated coefficient is the rate ratio change in the dependent variable (TIME2:PGBI-10M) corresponding to one unit change in the predictor variable.

Abbreviations: Time 1 Parental General Behavioral Inventory-10 Item mania scale (TIME1:PGBI-10M); Schedule for Affective Disorders and Schizophrenia for School-Age Children Mania Rating Scale (KMRS); Schedule for Affective Disorders and Schizophrenia for School-Age Children Depression Rating Scale (KDRS). VS = Ventral Striatum